An investigation of particle breakage in loess

Chongyang GAO
gaochongyang99@stu.xjtu.edu.cn
Department of Civil Engineering, School of human settlements and Civil Engineering, Xi'an Jiaotong University, Xi'an, Shannxi Province, China, 710054

Ling XU*
xuling82@xjtu.edu.cn
Department of Civil Engineering, School of human settlements and Civil Engineering, Xi'an Jiaotong University, Xi'an, Shannxi Province, China, 710054

Matthew Richard COOP
m.coop@ucl.ac.uk
Department of Civil, Environmental and Geomatic Engineering, University College London, U.K.

Chuang HUANG
hc1437243877@stu.xjtu.edu.cn
Department of Civil Engineering, School of human settlements and Civil Engineering, Xi'an Jiaotong University, Xi'an, Shannxi Province, China, 710054

Lu ZUO
zuol07@xjtu.edu.cn
Department of Civil Engineering, School of human settlements and Civil Engineering, Xi'an Jiaotong University, Xi'an, Shannxi Province, China, 710054

*Corresponding author

Abstract

The paper presents a detailed experimental investigation of particle breakage in three kinds of loess, i.e., sandy loess, silty loess and clayey loess. It is firstly found that particle breakage can occur within loess in oedometer test, which results in a better-graded soil at the end of the test. Initial breakage stresses for both the silty and clayey loess are less than 0.5 MPa, and about 2 MPa for the sandy loess. The relative breakage (B_r) is used to evaluate the particle breakage degree, and it is found that for all the three kinds of loess tested, B_r increases with the increasing loading stress until it reaches a threshold, after which B_r tends to keep a constant value. Particles within the loose specimens break more easily than those within the dense ones, especially for the sandy and silty loess. It is also observed that for the specimens reconstituted with previously tested soils, particle breakage degree decreases significantly, which means little particle breakage occurs in the pre-crushed specimens.

Keywords

Loess, Particle breakage, Compression, Soil grading

1. Introduction

Loess is a typical silt-sized soil (Liu, 1985). But it is a special soil with a bonded structure that is sensitive to rainfall, erosion, cyclic loading, and human activities (Peng et al., 2019). The mechanical behavior of loess has been extensively studied through laboratory tests, whereas there has been no investigation of its particle breakage. Virtually all investigations involving soil testing above normal geotechnical pressures have resulted in considerable particle breakage (Hardin,1985; Bishop,1966; Terzaghi and Peck,1948). For example, the particles at the bottom of a high dam or the tip of pile, especially during driving, or in the sliding zone of a landslide (Indraratna et al., 1998). In recent years, some geotechnical mega-projects have been carried out in the loess area of China such as the removal of the tops of mountains and infilling of valleys by compaction (Li et al., 2014). Particle breakage might occur in these cases. Hence an investigation of loess particle breakage is necessary to identify the engineering properties of such granular materials.

Particle morphology (shape, size, angularity, roundness, and the surface roughness etc.), particle composition (initial void ratio and gradation), loading conditions (state of effective stress, effective stress path) and the constituent minerals are the main influencing factors that affect the amount of particle breakage. The relationship between these factors and the soil crushing strength as well as the empirical correlations has been studied by many researchers (Zhang et al., 2019; Mehta and Patel, 2017; Xiao et al., 2017; Shahnazari and Rezvani, 2013; Altuhafi and Coop, 2011b; Erzin et al., 2012; Arasan et al., 2011; Feda, 2002; Lade et al., 1996). It was reported that the larger and angular particles in soil with less quartz percentage break more easily (Erzin and Yilmaz, 2008). And the stress state of sufficient magnitude is the key factor that determines the

quantity of particle breakage (Altuhafi and Coop, 2011b). The relative density of soil affects the inter-particle contacts and average contact stress, which in turn determines the crushing characteristics (Erzin and Yilmaz, 2008; Lade, et al. 1996).

Particle breakage alters the matrix of particle size distribution (PSD) and the pore size distribution (Mehta and Patel, 2018), which is directly linked to the engineering behavior of soils, such as the hydraulic conductivity (Valdes and Caban, 2006), stiffness (Fu et al., 2014), strength (Indraratna et al.,1998), dilatancy (Liu and Gao, 2016; Wang et al., 2019), and critical states (Bandini and Coop, 2011; Ghafghazi et al., 2014; Wood and Maeda, 2008; Coop et al., 2004). The above studies mainly focused on the particle breakage of sands, ballast, coal, rockfill and cemented soils. The loess soils are mainly composed of more silt-sized particles (0.005~0.075 mm) than the sands and other granular soils reported. The silt grains can be about 50-100% of the total weight, varying with locations in China (Liu, 1985). Recently, there are evidences showing that particle breakage occurs in silty-sized iron tailings (Li and Coop, 2019). It therefore raises questions whether the silts of loess will break down during loading and whether the crushed particles will affect the compression behavior of loess.

A series of oedometer tests were therefore conducted to explore loess particle breakage. Three loess zones have been identified in China, namely the sandy, silty and clayey loess zones according to the PSD. The loess specimens used in this study were retrieved from Yulin city (the sandy loess zone), Lanzhou city (the silty loess zone) and Xi'an city (the clayey loess zone), respectively. The sampling locations are shown in Fig. 1. Note that the clayey loess is actually finer silty loess though it was retrieved from the clayey loess zone. Although it does have more clay-sized particles than the silty and

sandy loess, it is still composed predominantly of silts (Fig. 2). A laser particle size analyzer was used in the study to identify the particle breakage through capturing the variations of PSD. This method avoids human interference to the greatest extent possible. In addition, the required quantity of soil is small.

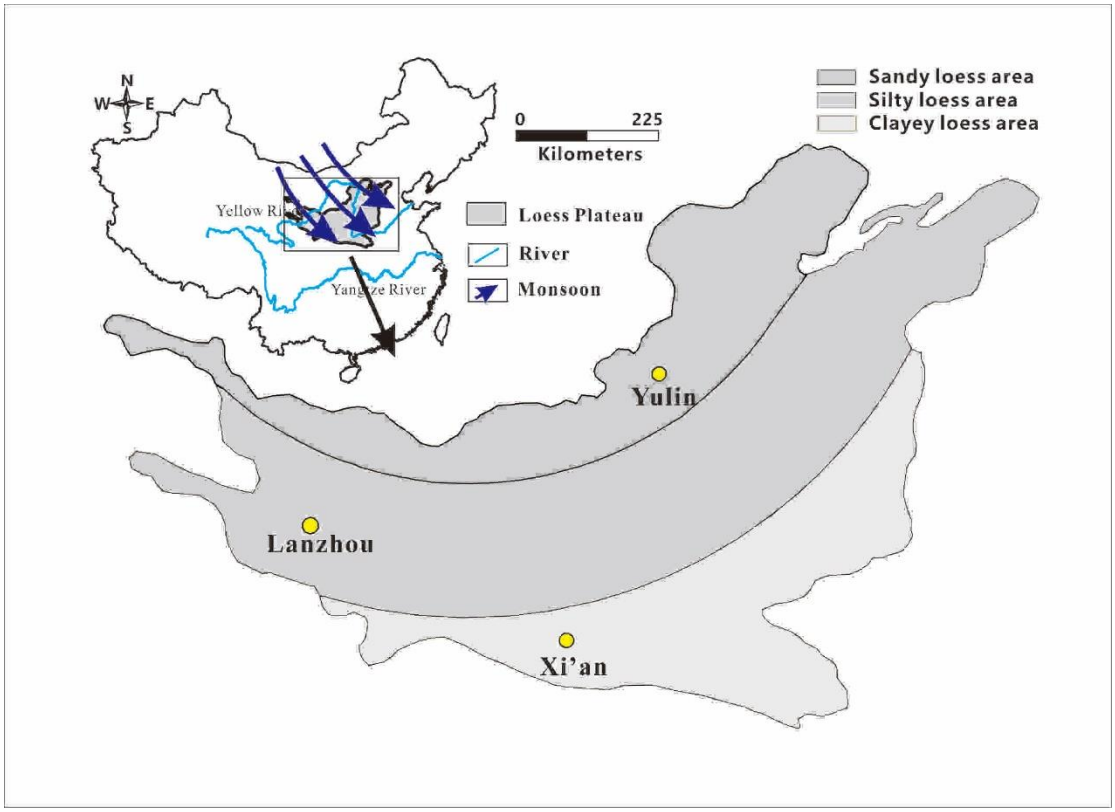

Fig. 1 Sampling sites on the loess plateau of China

2. Materials and Methods

Fig. 2 presents the PSD curves of the loess before testing. The results were obtained with a Mastersizer 2000 laser diffractometer. For each soil, an average value of three parallel measurement results was used to capture the soil particle size accurately. The percentages of fine particles (less than 0.005 mm) are about 2.2%, 3.7% and 20.1% for sandy loess of Yulin, silty loess of Lanzhou and clayey loess of Xi'an, respectively.

The index properties for the three materials are presented in Table 1. The specific gravity of the loess is about 2.68 ~ 2.73. The coefficient of uniformity C_u and the coefficient of curvature C_c that characterize the shape of the PSD curve are expressed in Eq. (1) and Eq. (2). Fig. 3 shows the plasticity chart for the soils. The clayey loess has a medium plasticity while the sandy and silty loess have a low plasticity. Fig. 4 shows the mineral compositions of the samples. The main mineral components are quartz, albite, calcite and clay minerals for all tested materials. From the sandy loess to the clayey loess, the contents of quartz and albite decrease while the calcite and clay minerals increase with the increasing proportion of fine particles.

$$C_u = \frac{D_{60}}{D_{10}} \quad (1)$$

$$C_c = \frac{D_{30}^2}{D_{60} D_{10}} \quad (2)$$

where the C_u is coefficient of uniformity, C_c is the coefficient of curvature, D_{10}, D_{30} and D_{60} are the particle diameters at 10%,30%, and 60% of passing mass of soil.

Oedometer tests were carried out to investigate the particle breakage under loading. The maximum vertical stress applied ranges from 0.1 to 35 MPa. The height and diameter of the oedometer ring were 20 mm and 50 mm, respectively, except in the 35 MPa tests, for which the height and diameter were both 20 mm. It was demonstrated that the sample size has negligible effect on particle breakage by analyzing the PSDs of samples with 20 mm and 50 mm diameter cells before and after tests. All the reconstituted specimens were prepared using the wet compaction method at a water content of about 10% by weight. The wet soil was mixed evenly and then compacted by 3 layers in a

split mold. The compaction hammer weighs 570 g and falls from 20 cm height above the top of the ring. After the specimens were prepared, vacuum saturation method was adopted to saturate the specimens. Then the specimens were loaded in stages to reach the chosen maximum vertical stress. The specimen deformation is related to the content of clay particles as well as the applied stress level. The end standard of the consolidation test in this study is that the deformation within 1 hour is less than 0.01 mm to avoid creep (Leung et al., 1996; Takei et al., 2001). For the loess specimens with a vertical loading stress of less than 1 Mpa, 4 hours are enough to reach the end standard. For the tests that the maximum vertical loading of 35 MPa is applied, 16 hours of loading are needed. The oedometer cells were filled with water to make certain that all suctions were dissipated. At the end of each test, unload to the final stage of 12.5 kPa and maintain no less than 12 hours. After fully unloaded, the final water content of specimens was measured. The initial specific volume v_i equals to 1+e was calculated by two independent ways, as shown in Eq. (3) and Eq. (4), from the initial specimen volume and final water content measurements. An average results of these two methods was taken. The tests with the two specific volume values with difference greater than 0.04 were discarded.

$$v_i = \frac{G_s \gamma_w (1 + w_i)}{\gamma_i} \tag{3}$$

$$v_i = \frac{G_s w_f + 1}{1 - \varepsilon_v} \tag{4}$$

where the G_s is the specific gravity, γ_w is the unit weight of water, γ_i is initial bulk unit weight, w_i and w_f are the initial and final water contents, and ε_v is the volumetric strain.

Particle breakage during oedometer compression is characterized by capturing the PSDs before and after tests, respectively. In this study, three aspects of particle breakage have been investigated. Firstly, the relationship between particle breakage and the maximum applied vertical stress was studied. In order to eliminate the influence of soil density, efforts were made to create specimens with a given initial void ratio. Secondly, influence of soil initial density on the particle breakage has been identified. To avoid particle breakage in the process of specimen preparation, as pointed out by Sun et al. (2019), the specimens were not compacted to extreme densities. The PSDs of the soils before and after specimen preparation were examined. The results indicated that there was no particle breakage in the specimen preparation. Lastly, to explore the influence of repeated loading on the soil particle breakage, some pre-crushed specimens were remolded and tested again. To provide enough soil materials for the pre-crushed specimen preparation, at least three parallel oedometer tests were carried out under the same conditions. The pre-crushed specimens were then prepared by reconstituting the specimens that had been tested. The first-level pre-crushed specimens were prepared using the tested specimens of uncrushed loess (natural loess). Second-level pre-crushed specimens were prepared using the first-level pre-crushed specimens after testing.

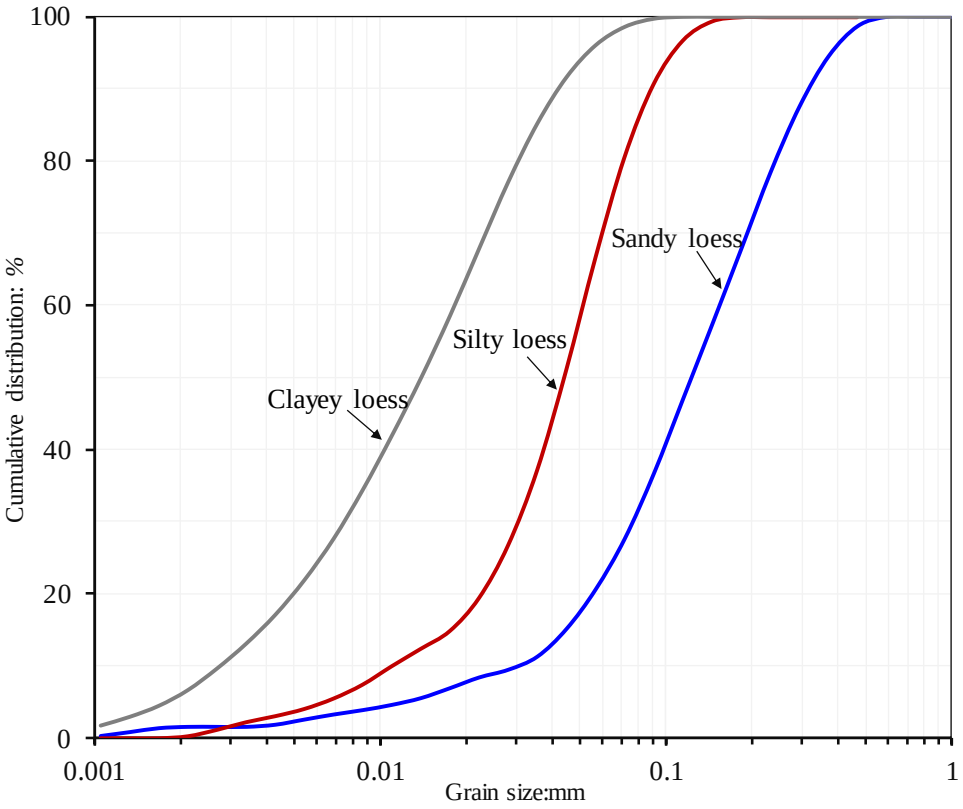

Fig. 2 Initial PSD of the loess soils

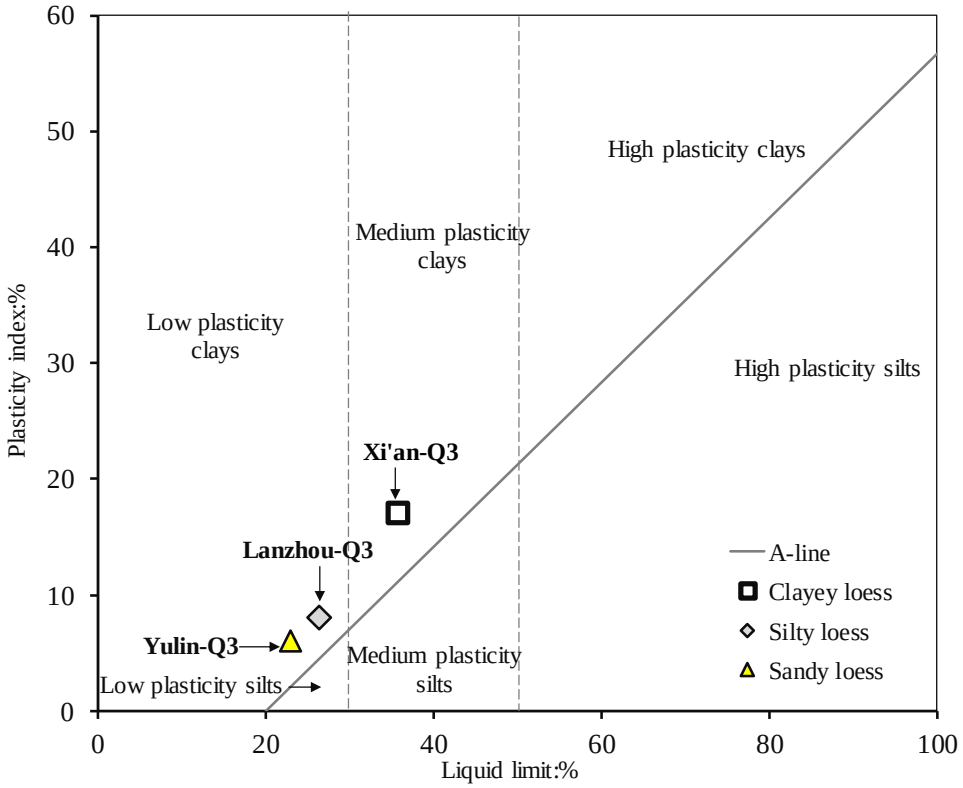

Fig. 3 Casagrande classification chart for the specimens

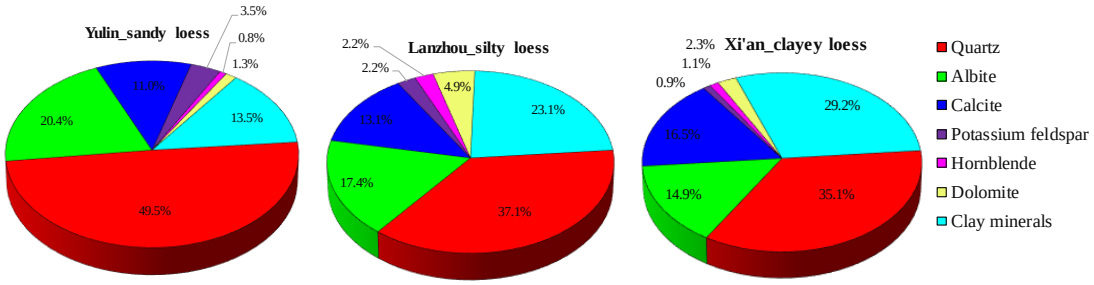

Fig. 4 Mineralogical compositions of the loess

Table-1 The index properties of the loess

Type of soil	Sampling location	G_s	Liquid Limit (LL)	Plasticity Index (PI)	Percentage finer(<5μm)	C_u	C_c
Sandy loess	Yulin	2.68	22.9	6.0	2.2%	4.95	1.22
Silty loess	Lanzhou	2.73	32.0	19.8	3.7%	3.71	1.21
Clayey loess	Xi'an	2.72	25.3	4.9	20.1%	6.64	1.12

Table-2 Details of the oedometer tests

Loess type	Test number	Sampling location	Preparation method	Initial specific volume: v_0	$\sigma_{v'max}$ (MPa)	Final specific volume: v_f
Sandy loess	01	YL	WC	1.719	5.6	1.415
	02	YL	WC	1.753	15	1.311
	03	YL	WC	1.742	0.5	1.581
	04	YL	WC	1.736	2	1.519
	05	YL	WC	1.598	2	1.497
	06	YL	WC	1.803	3	1.472
	07	YL	WC	1.499	5.6	1.403
	08	YL	WC	1.543	15	1.365
	09	YL	WC	1.405	18	1.330
	10	YL	WC	1.469	25	1.348
	11	YL	WC	1.504	35	1.328
	12	YL	WC	1.718	35	1.324
	13	YL	WC	1.780	4	1.456
	14	YL	WC*	1.783	4	1.457
	15	YL	WC**	1.772	4	1.448
Silty loess	16	LZ	WC	2.116	4	1.709
	17	LZ	WC	2.053	15	1.517
	18	LZ	WC	1.937	0.5	1.772
	19	LZ	WC	2.022	1	1.752
	20	LZ	WC	1.714	1	1.654
	21	LZ	WC	1.966	2	1.696
	22	LZ	WC	2.054	4	1.637
	23	LZ	WC	1.799	4	1.620
	24	LZ	WC	1.823	10	1.543

	25	LZ	WC	1.987	15	1.483
	26	LZ	WC	1.694	15	1.485
	27	LZ	WC	1.762	25	1.466
	28	LZ	WC	1.787	35	1.439
	29	LZ	WC	1.943	35	1.366
	30	LZ	WC	2.066	4	1.639
	31	LZ	WC*	1.968	4	1.616
	32	LZ	WC**	1.946	4	1.600
Clayey loess	33	XA	WC	2.042	1.6	1.480
	34	XA	WC	2.096	5	1.411
	35	XA	WC	2.083	15	1.325
	36	XA	WC	1.986	0.1	1.820
	37	XA	WC	2.073	0.5	1.632
	38	XA	WC	2.086	1	1.559
	39	XA	WC	1.650	1	1.558
	40	XA	WC	1.986	1.6	1.484
	41	XA	WC	0.931	2	0.493
	42	XA	WC	2.577	4	2.131
	43	XA	WC	1.570	5	1.385
	44	XA	WC	1.660	15	1.315
	45	XA	WC	1.920	30	1.309
	46	XA	WC	1.910	4	1.419
	47	XA	WC*	1.953	4	1.432
	48	XA	WC**	1.849	4	1.400

Notations: YL, Yulin; XA, Xi'an; LZ, Lanzhou; WC, wet compaction; WC*, the first level pre-crushed specimen by compaction method; WC**, the second level pre-crushed specimen by compaction method.

3. Test results and analysis

3.1. Influence of stress level on particle breakage

Fig. 5 presents the results of tests in which the maximum vertical stresses applied were different. It shows that the three types of loess have different shapes in their compression paths and one-dimensional normal compression lines (1D-NCLs). Although the clayey loess has low clay content, its compression path is more like that of a clay soil. The compression path reaches its 1D-NCL at only a few tens of kPa, and the 1D-NCL is concave upwards. With the increase of coarser particles, the slopes of 1D-NCL (compression index) of clayey loess, silty loess and sandy loess reach 0.09,

0.13 and 0.09, respectively. The compression paths of silty loess at the end of the tests are even above the clayey loess though the latter had the loosest initial density. The silty and sandy loess show a typical sandy or silty mode of behavior as expected, where the compression curves are convex upwards and then reach a unique 1D-NCL only at high stresses. In these cases, the loess tends to a higher compressibility at higher stresses after experiencing an initially low compressibility. The yield of the sandy and silty loess is very gradual, in contrast to poorly graded sands, but which is typical for better graded silty soils (Vilhar et al., 2013).

Fig. 6 presents the PSDs of the soils before and after testing, respectively. The applied maximum vertical stresses for the oedometer tests are labelled. The PSDs of the soils after testing are clearly different from those before the test. For the clayey loess, the significant particle breakage seems to commence at about 0.1 MPa ~ 0.5 MPa, while for the sandy loess it starts at about 2 MPa ~ 3 MPa. For the silty loess, the lowest maximum vertical stress applied was 0.5 MPa, for which the particle breakage was already significant. With further increases of the maximum vertical stress, there is more particle breakage.

From Fig. 6, at higher stresses the particle breakage of the clayey loess is clearly less than that of silty loess. The latter is then less than that for the sandy loess. This is consistent with the dependence of breakage on particle size identified by McDowell et al. (1996), even if the stress at which that breakage starts is not the same. Detailed comparisons cannot be made as there are differences of grading uniformity and of mineralogy among the various soils. For example, the sandy loess has a similar grading to an alluvial silty sand tested by Vilhar et al. (2013). But the breakage of sandy loess

is very much greater.

More details about the size of the particles broken in the test can be found in Fig. 7, which presents the density distributions of different sized particles in the specimens before and after testing. It is observed that the tested silty loess has a distribution that keeps the peak at about the same point, while for the sandy loess the peak migrates to the left and for the clayey loess the peak migrates slightly to the right although the clayey loess cannot cross the initial grading, of course, so it is constrained. The main particle sizes that are broken in the sandy, silty, and clayey loess are about 0.1~0.6 mm, 0.03~0.1 mm and 0.007~0.025 mm, respectively. These particle size ranges do not overlap with each other, reflecting the particle breakage dose not significantly change the PSDs of tested loess. The new finer particles generated due to breakage mainly accumulate in the sizes of 0.001~0.15 mm, 0.001~0.03 mm and 0.001~0.007 mm for the sandy, silty, and clayey loess respectively. It seems that the coarser particles break into a wider range of finer particles.

It is interesting to observe where the breakage occurs in each soil. In the clayey loess, the coarser particles of 0.025-0.08 mm the percentage of which is 21%, did not break much. However, this size range is mostly prone to break in the silty loess. In contrast with the sandy loess, the particle sizes of this range probably did not break much as there is an accumulation in this size range. However, this does not mean that there is no breakage in the size range although the accumulation is greater than any breakage. The large-scale breakage of sandy loess was predominantly in the coarser particle fraction. Herein, as the grading of samples gradually change from sandy loess, silty loess to clayey loess, the breakage within each soil moves towards the finer fraction of each soil.

These observations for the sandy loess contrast what has been observed in poorly-graded sands, where the breakage occurs preferentially in the finer gradings, leading to a tendency towards fractal gradings (McDowell and Bolton, 1998). Although in gap graded soils, similar breakage in both the coarse and fine fractions has been observed in sandy loess (Zhang et al., 2017).

Fig. 8 shows the SEM images before and after tests, respectively, illustrating the particles and their arrangement in the specimens. Generally, the mean particle size of the specimens after test are smaller than those prior to loading though the soil density after test is much larger than that before test. For the sandy loess, it is clear that the particles with dimensions larger than 100 μm decrease due to particle breakage. In these cases, the particle fractures can be clearly seen but the pieces still remained in close proximity to each other. The coarse particles were originally irregular in shape with some angular corners which may have generated their breakage (Erzin and Yilmaz, 2008). For the silty loess, the particles with dimensions larger than 50 μm decrease due to particle breakage. For the clayey loess, the change is not obvious. This is mainly because that particle breakage is very small and the soil experienced a more significantly compression. In this case, it is much difficult to identify particle size variations from SEM image observations. Some large particles can also be seen in the clayey loess, immersed in a matrix of greatly increased fines. It is evident from the SEM images that some of the particles are aggregated fines, which is easy to break once the vertical loading was applied. However, the grading changes would not reflect the aggregate breakages because the laser diffractometry method requires the specimen to be stirred in a water bath which would break them up.

Based on the PSDs (Figs. 6 and 7) and the SEM images (Fig. 8), three micro-fabric models for the clayey loess, silty loess and sandy loess are proposed as illustrated in Fig. 9. For the clayey loess, the percentage of fine particles (<0.025 mm) are 70%. The coarse particles (>0.025 mm) are largely isolated by the matrix of fine particles (Fig. 9a) and may not form a percolating system. Herein, the force transmission is through the contacts between the fine particles and contacts between the fine particles and the coarse particles or fines aggregates. Consistently with McDowell and Bolton (1998), for a given vertical stress, the higher coordination number of the large particles allows them to survive. As the stress increases, the content of large-sized particles in the clay loess does not change significantly referring to the particle size between 0.025 and 0.08 mm, rather than continuous to decrease. For the particles in these size ranges, with the increase of loading stress, the variations of particle breakage can be neglected. For the silty loess, the percentage of fine particles (<0.03 mm) are less than 25%, while the coarse particles of silts (0.03-0.075 mm) and sands (0.075-0.08 mm) make up about 58% and 17%, respectively. For the sandy loess, the percentage of sand particles (0.075-0.6 mm) is 72%. As the coarse particle content increases from the clayey, silty to sandy loess, it forms a percolating system with the fines increasingly in the between voids so that the breakage shifts towards the coarser fraction.

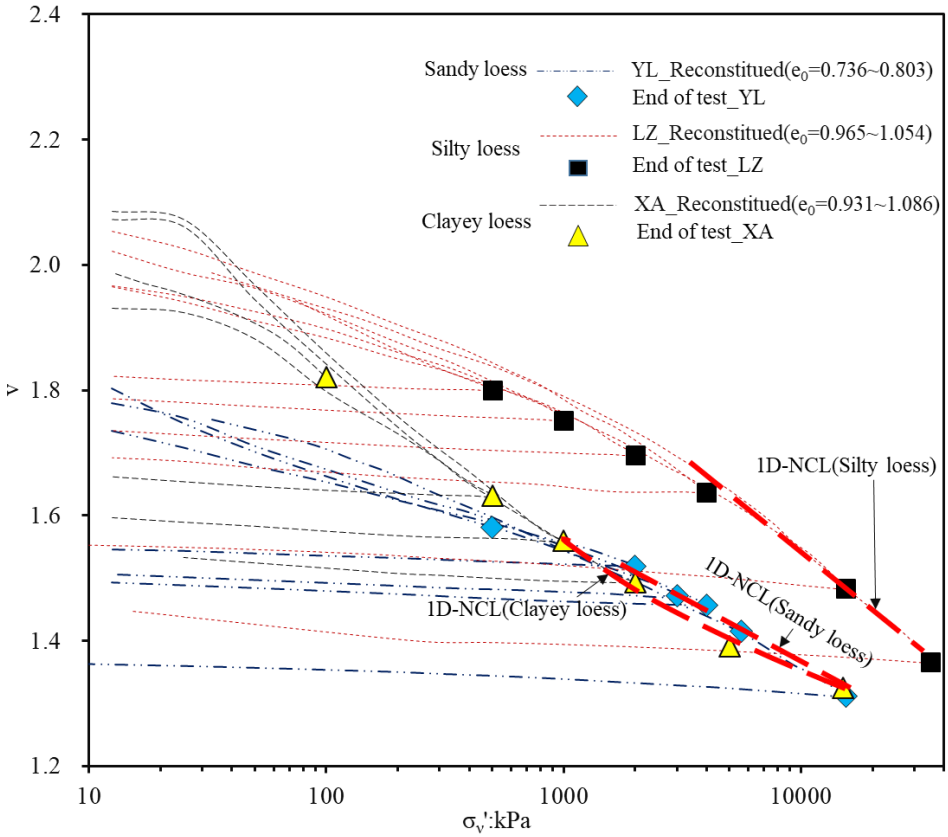

Fig. 5 The compression curves obtained from the oedometer tests

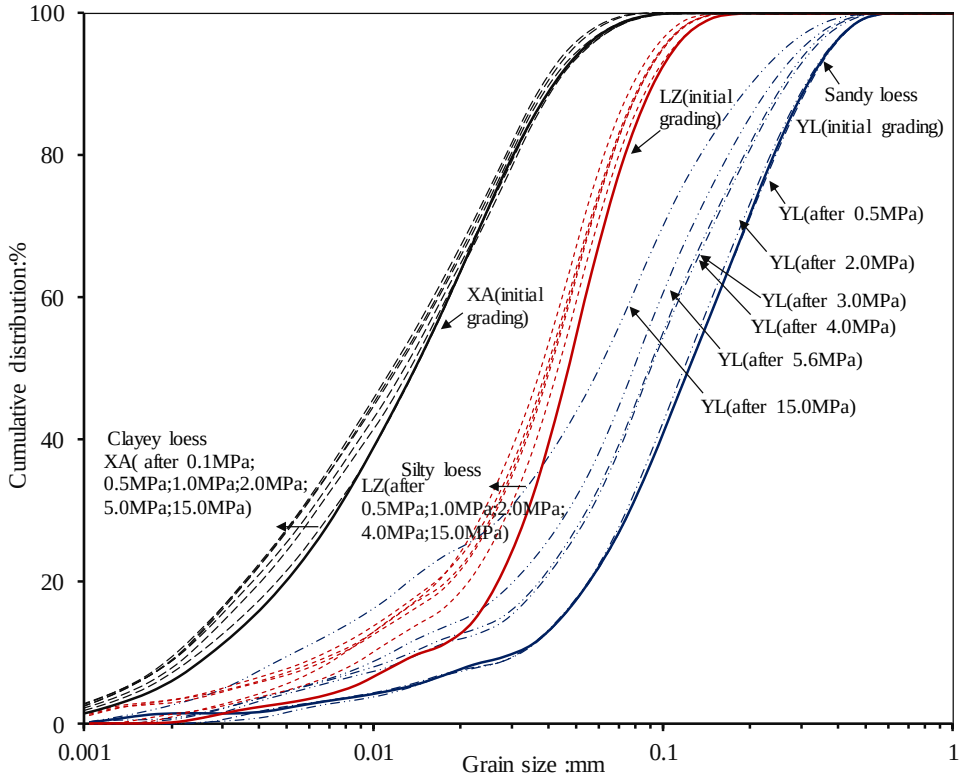

Fig. 6 PSD curves of the loess in initial condition and after testing

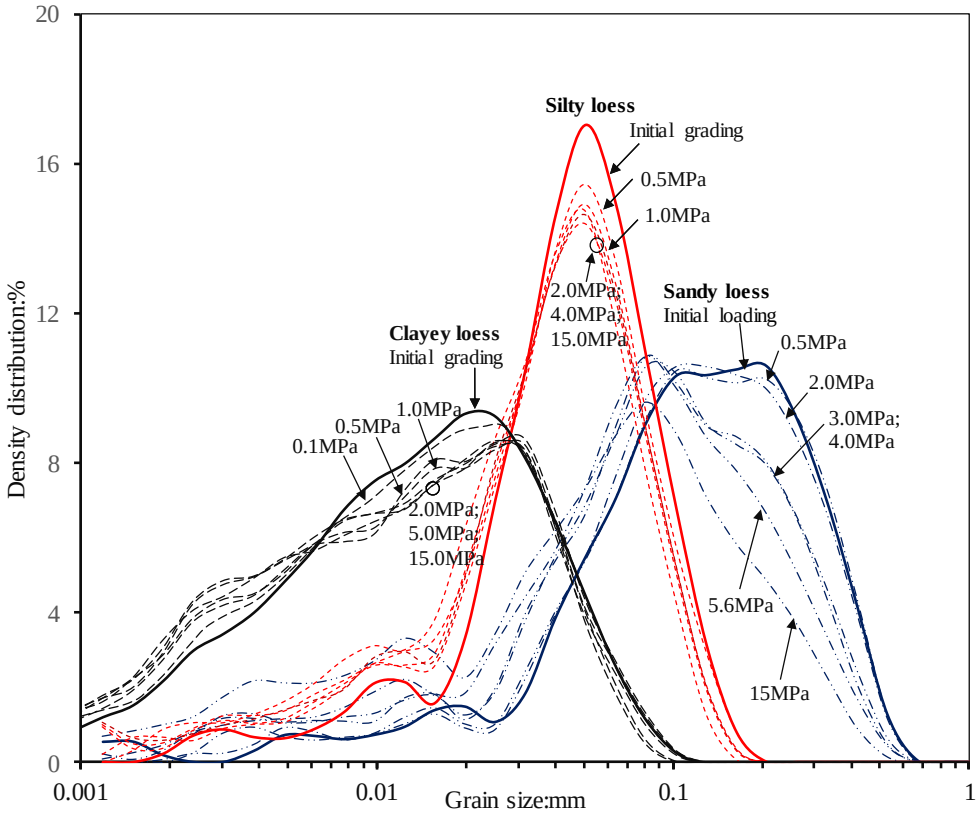

Fig. 7 Density distributions of particle sizes before and after testing

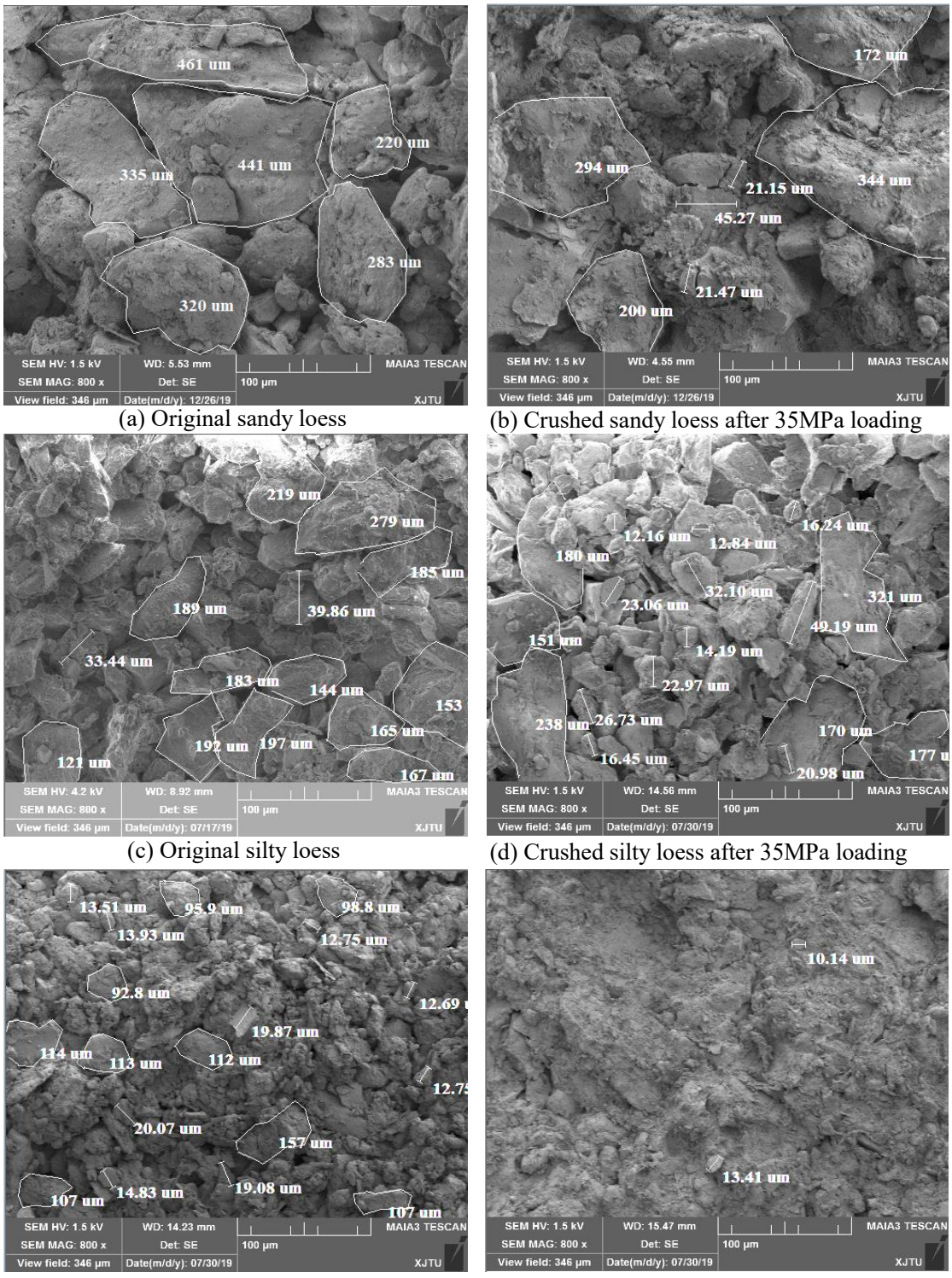

(a) Original sandy loess (b) Crushed sandy loess after 35MPa loading

(c) Original silty loess (d) Crushed silty loess after 35MPa loading

(e) Original clayey loess (f) Crushed clayey loess after 35MPa loading

Fig. 8 SEM images of the original soils and crushed soils after 35 MPa vertical loading stress of Yulin sandy loess, Lanzhou silty loess and Xi'an clayey loess

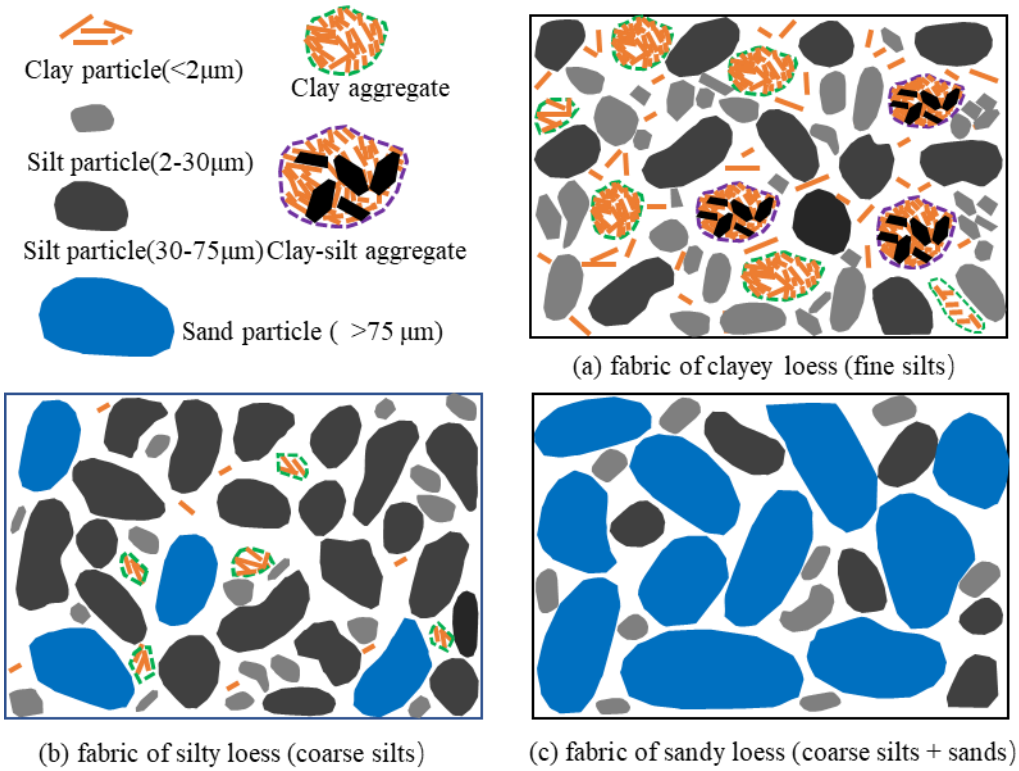

Fig. 9 Fabric models proposed for three loess soils

The relative breakage (B_r) developed by Hardin (1985) as illustrated in Fig. 10 is a commonly used parameter to quantify the particle breakage, which is adopted in this study. The assumption that the finest particles don't contribute to the breakage has been verified in this particle breakage analysis. However, Hardin had a cut off at 0.074 mm because he used sieving while in this study it is clear that the finer particles break. For rock minerals, the comminution limit is in the order of 1 μm and the particles of less than 1 μm is neglectable (Vilhar et al., 2013). For the tested loess, their particles are even coarser than the rock materials, of which the particles size of less than 2 μm are neglectable. In this study, 2 μm was taken as the crushing limit to define B_r.

Fig. 11 shows the results of B_r versus the maximum vertical stress applied in the oedometer tests, the compression paths of which were presented in Fig. 5. As discussed

above, the initial stress that caused the particle breakage is less than 0.5 MPa for the clayey and silty loess, and less than 3 MPa for the sandy loess. Once breakage commences, B_r increases rapidly with increasing stress initially. However, after about 2 MPa, the B_r of the clayey and silty loess tend towards more constant values, or at least the breakage decelerates rapidly, with much less further breakage in the specimen. The B_r value at 30 MPa for the clayey loess decreases due to some small experimental scatter. The slowing down of the breakage occurs because of the increase of coordination numbers due to the large increase of the numbers of finer particles. For the sandy loess, the B_r value continuously increases though it tends to increase more slowly when the maximum vertical stress of 35 MPa was applied. This may be due to that sandy loess has a higher proportion of quartz, which is a mineral with greater strength (Fig. 4), while the silty and clayey loess have higher proportions of feldspars (albite and potassium) along with calcite/dolomite, which are all weaker minerals (Nakata et al., 1999). On the other hand, these differences may also be linked to the predominance of breakage in different parts of the PSD.

The input specific work, W is introduced here to explore the factors to influence B_r. According to the experimental conclusion of Indraratna and Salim (2002), the total input energy should eventually be converted to particle rearrangement, particle friction and particle breakage energy consumption. The W can be calculated with the integration, as shown in Eq.(5)

$$W=\int \sigma_a^{'} \mathrm{d}\varepsilon_a \tag{5}$$

where $\sigma_a^{'}$ is the vertical stress and ε_a is the axial strain.

346 The input specific work is calculated from the vertical stress at the beginning of test as
347 the starting point, until the end of test. The relationship between B_r and W during
348 the compression process is presented in Fig. 12. With the increase of the W, the B_r
349 increases non-linearly, which has also been validated by many researchers (Xiao et al.,
350 2019;Huang et al., 2014). The law of B_r and W is consistent with that of B_r and
351 the maximum vertical stress, indicating that the input work of the samples with similar
352 initial void ratio is mainly affected by vertical stress during the loading process. At the
353 initial stage, the clayey loess and silty loess have a higher B_r value than that of the
354 sandy loess. It indicates that the clayey loess and silty loess are easier to break than the
355 sandy loess. But with the increasing W, the B_r approximately reaches a constant
356 value.
357
358 Relative breakage B_r has a significant advantage of representing the overall amount
359 of breakage as a single parameter. But it does not consider the differences of soil grading
360 or the characteristics of the grain-size distribution (Yu et al., 2019). In this study, the
361 interacting effects of soil grading on particle breakage and the influence of particle
362 breakage on grading were identified. Two parameters, the mean particle size (D_{50}) and
363 the coefficient of uniformity (C_u), have been used to define the PSD. Fig. 13 presents
364 the relationships among B_r, D_{50} and C_u of the specimens after compression. In Fig.
365 13a, after particle breakage, D_{50} follows a unique relationship with B_r for each soil.
366 Even for the clayey loess, the variation of D_{50} is very small because the breakage in
367 the clayey loess was mainly for the particles with sizes less than D_{50}. The overall effect
368 for D_{50} of the three soils is to converge with each other. Fig. 13b shows the

relationships between B_r and C_u of the specimens after testing. The particle breakage generally leads to the C_u increasing in an approximately linearly relationship, indicating that the soils become better graded. Within some scatter, this relationship is unique for the three soils.

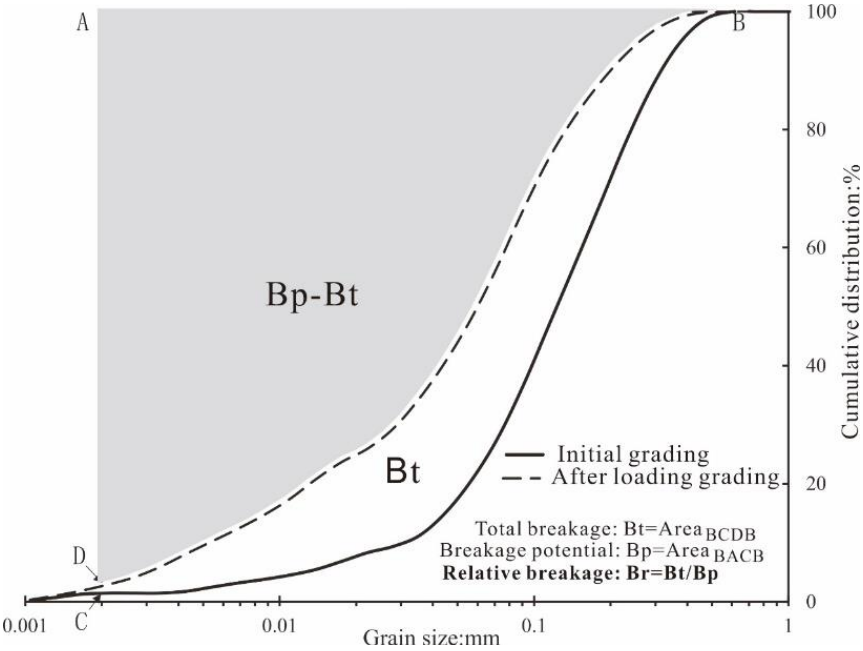

Fig. 10 Definition of the relative breakage B_r, modified from Hardin (1985)

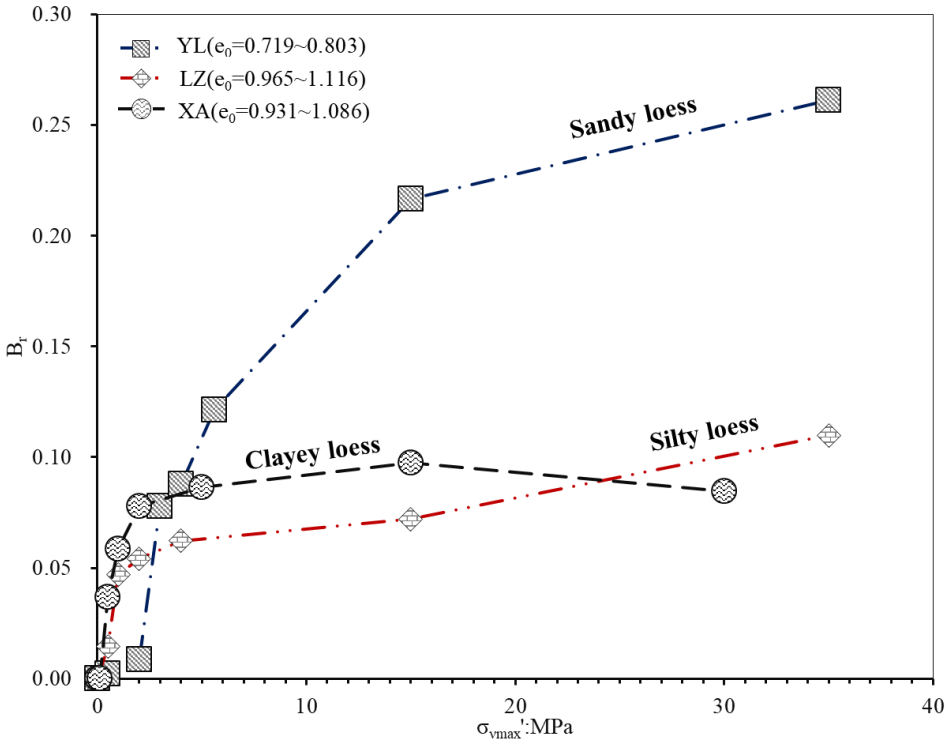

376

377 Fig. 11 Relative breakage B_r of the specimens compressed to different stress levels

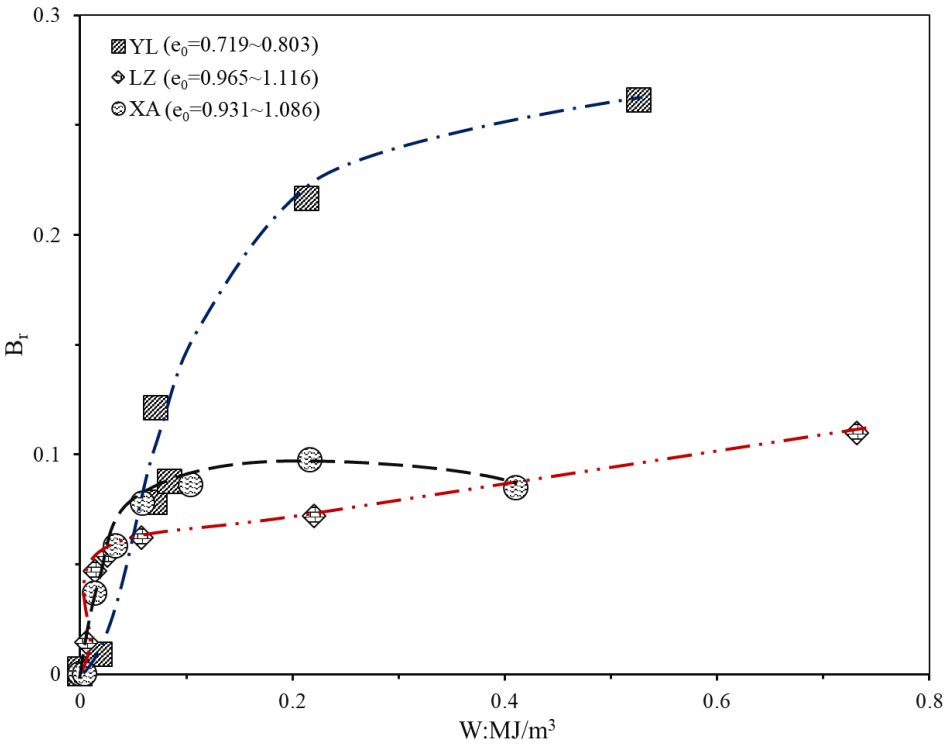

378

379 Fig. 12 The relationship between B_r and W during the compression process

380

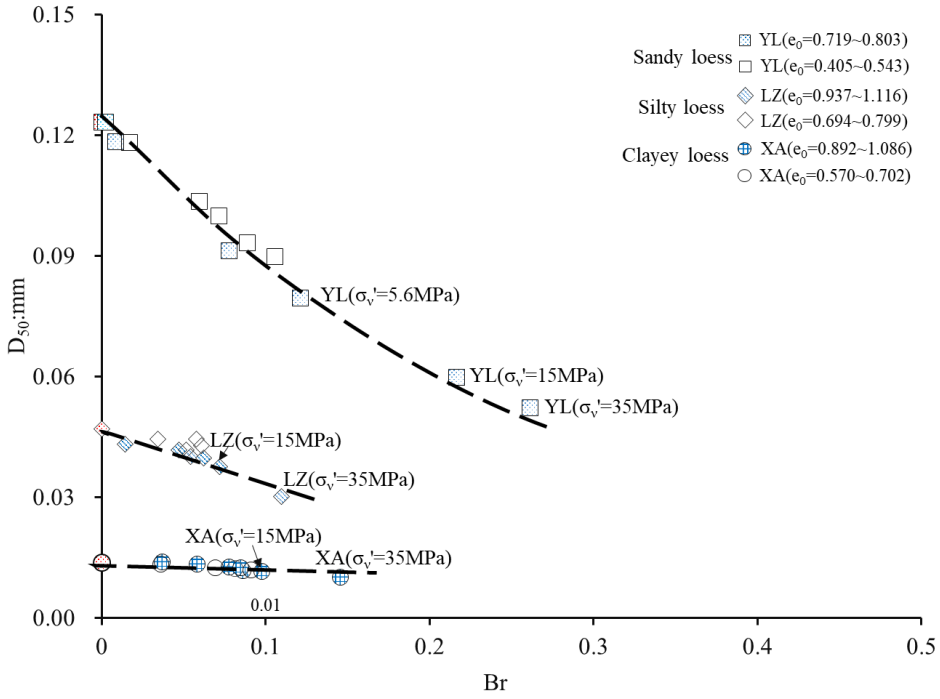

(a) B_r against D_{50} after compression

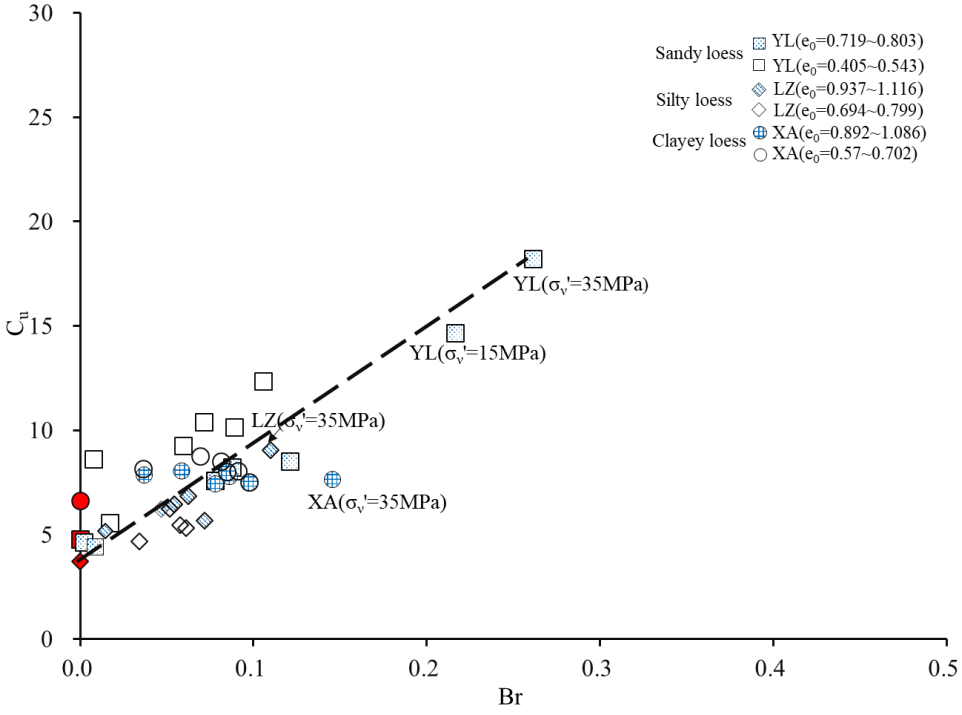

(b) B_r against C_u after compression

Fig. 13 The effect of particle breakage on the soil grading after compression

3.2. Influences of specimen density on particle breakage

Fig. 14 shows the compression curves of specimens with different initial void ratio. In

order to identify the influence of initial density on particle breakage, the PSDs of specimens were compared before and after testing. The results are presented in Fig. 15. For the specimens of dense sandy loess, e.g. YL (σ'_v = 5.6 MPa, e_0 = 0.499), the PSDs after tests are very close to the initial one. While for the loose specimens, e.g. YL (σ'_v = 5.6 MPa, e_0 = 0.719), coarser particles broke and a significant difference of the PSDs of the dense specimens was found. At larger stresses, the particle breakage in the loose specimen, e.g. YL (σ'_v = 35 MPa, e_0 = 0.718), is much more significant than in the dense one, e.g. YL (σ'_v = 35 MPa, e_0 = 0.504). In fact, the particle breakage in the loose specimen at a low vertical stress, YL (σ'_v = 5.6 MPa, e_0 = 0.719), is much more than that of the dense specimen at a higher stress, YL (σ'_v = 35 MPa, e_0 = 0.504). These differences reflect the key importance of coordination number on breakage (McDowell and Bolton, 1998). Similar conclusions were found in the silty and clayey loess, as can be seen in Fig. 16.

Fig. 17 shows the relationship between B_r and W of samples. It shows the greater the input energy is, the higher the relative breakage will be. For the sample LZ (σ_V=4.0 MPa) shown in Fig. 17 appears to be contrary to this conclusion, which may be due to the small difference in the initial density as well the uncertain errors. Seen from the Fig. 17, the loose samples experienced a bigger input work than the dense samples. The total input energy should eventually be converted to particle rearrangement, particle friction and particle breakage energy consumption (Indraratna and Salim,2002). Only the particle breakage energy consumption is related to the amount of particle breakage. The higher energy consumption in the loose sample is also composed of the more significant particle rearrangement with comparison of the dense sample. The different particle fabrics in the loose and dense samples, such as there are more point-to-point contacts

414 in the loose sample, can also cause the difference in particle breakage.

415

416 Fig. 18 shows the detailed results of sizes of broken particles. For the sandy loess (YL),
417 the particle breakage of the loose specimens mainly concentrates in the coarser particles
418 (0.15 ~ 0.55 mm). While under the same stress, the sizes of the broken particles in the
419 dense specimens are slightly different at the range of 0.15~0.25 mm. After breakage,
420 the peak of loose specimens moves more significantly to the left and the distribution
421 becomes more peaked. While for the dense ones, the original flatter shape of density
422 distribution is largely maintained with a smaller leftward translation of the peak. For
423 the silty loess (LZ), the particle breakage of the loose specimens mainly concentrated
424 in the particle sizes of 0.04 ~ 0.18 mm, e.g. LZ (σ'_v = 1 MPa, e_0 = 1.022). But for the
425 dense specimen at the same maximum vertical stress, e.g. LZ (σ'_v = 1 MPa, e_0 = 0.714),
426 the particle breakage concentrates in the sizes of 0.04 ~ 0.07 mm, which is consistent
427 with the sandy loess. However, for the silty loess, the shape of the density distribution
428 changes much less with density than for the sandy loess. For the clayey loess, while
429 density does have a small effect on the quantity of breakage, it does not have a
430 consistent influence on the particle sizes being broken.

431

432

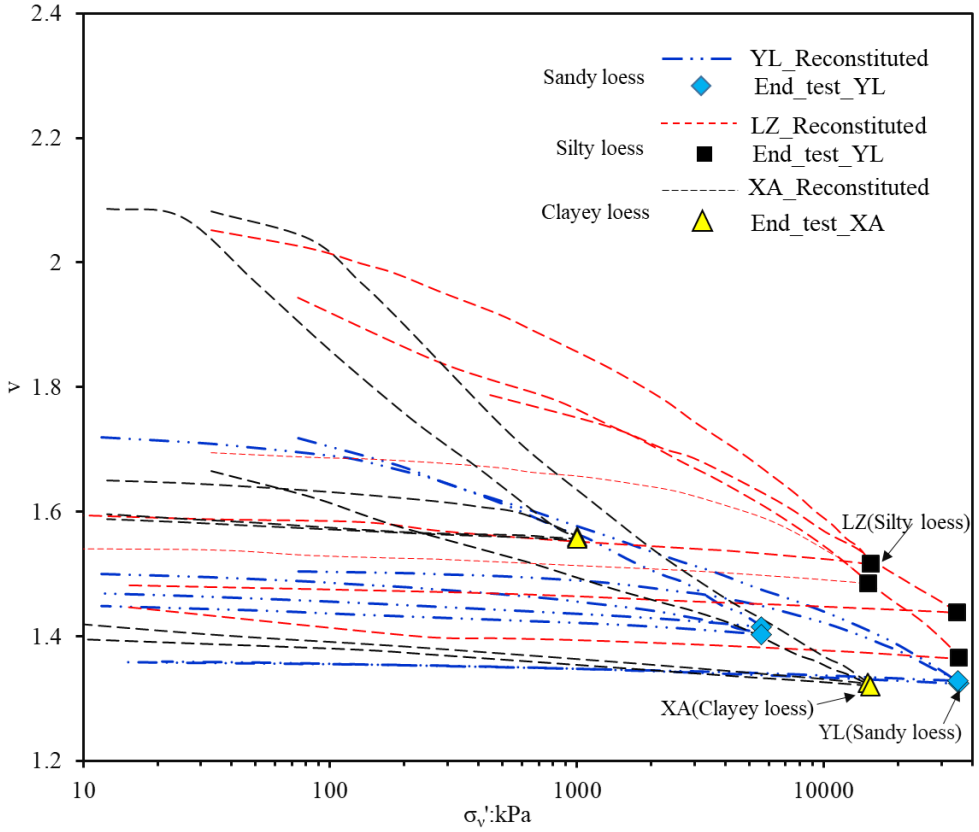

Fig. 14 The compression curves of specimens of different initial void ratio

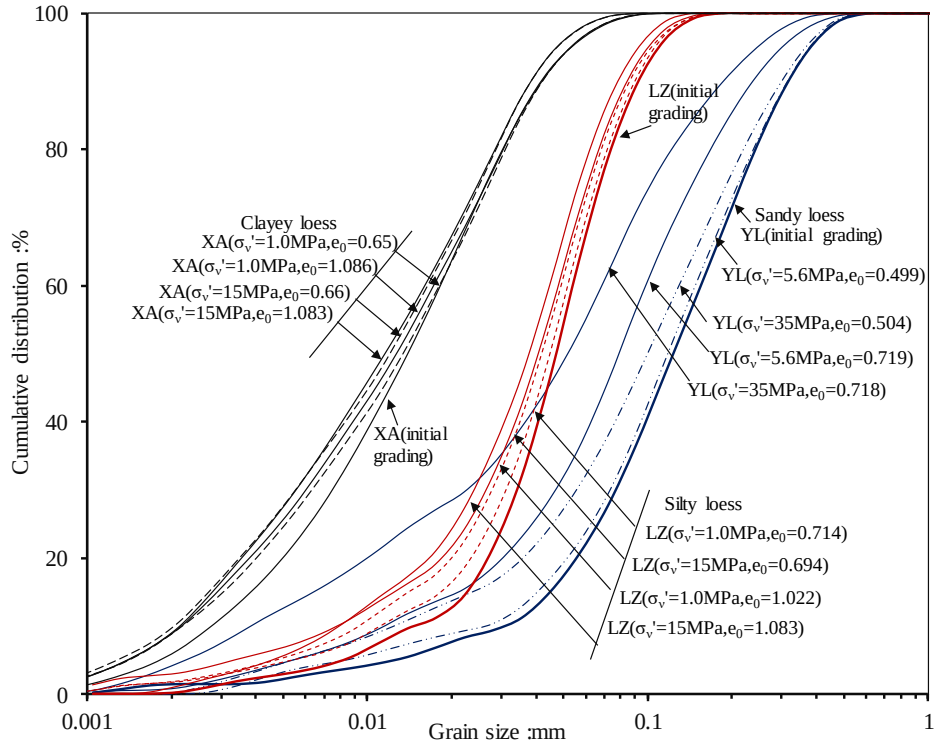

Fig. 15 PSDs for specimens of different initial densities before and after testing

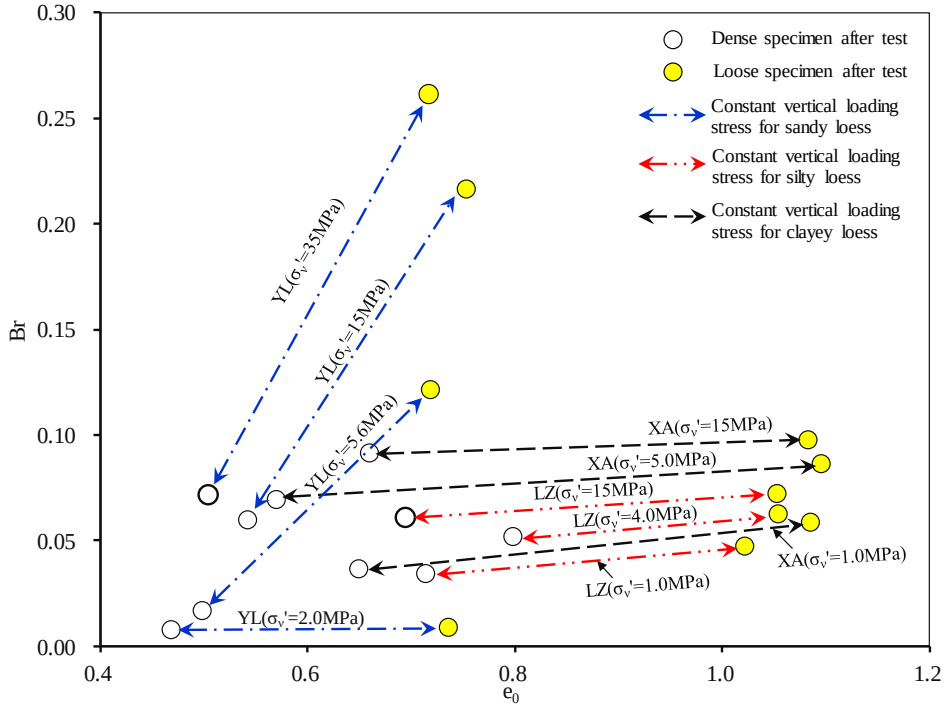

439

440 Fig. 16 Relative breakage B_r for specimens of different initial void ratios

441

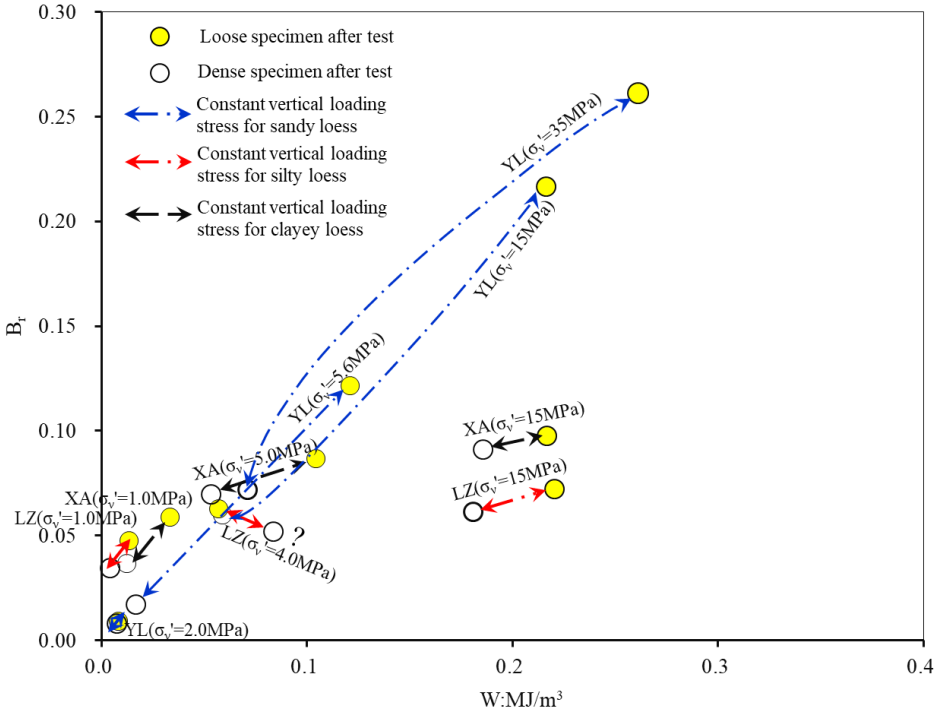

442

443 Fig. 17 The relationship between B_r and W of samples with different initial void

444 ratios

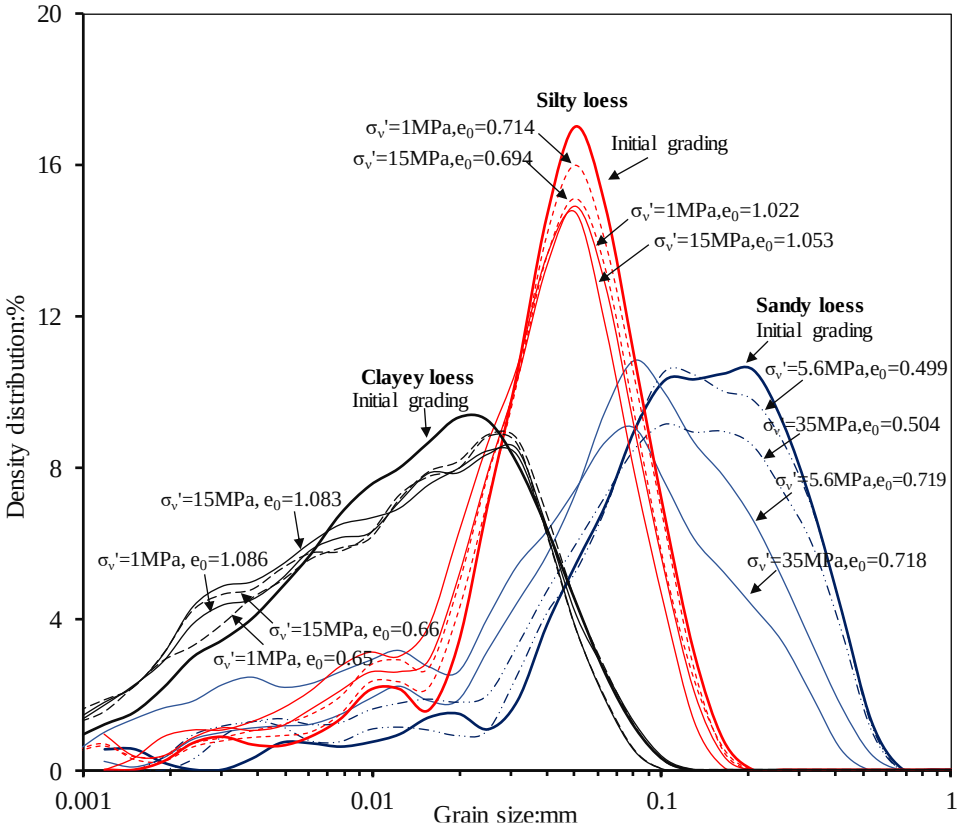

Fig. 18 Density distributions of particle sizes for specimens of different initial densities before and after testing

3.3. The particle breakage of pre-crushed specimens

Oedometer tests were carried out to study the particle breakage of pre-crushed specimens as shown in Fig. 19. Note that the pre-crushed specimens were made using the already tested samples by wet compaction method. For each soil, the specimens were prepared with the same initial void ratio. For the clayey loess, the compression paths of the various specimens had different yield stresses, then eventually converge. The compression paths for the silty loess do not converge and simply preserve small initial differences of specific volume. Even if there was only a very small measurable particle breakage in the second-level pre-crushed specimen (Fig. 20), the compression curve was still similar to that of the first-level pre-crushed specimen. For the sandy loess, the three specimens follow almost identical compression curves. It seems that the

influence of particle breakage on the compressibility of the silty and sandy loess is very small.

Fig. 20 shows the PSDs of the soils before and after testing, respectively. For the natural uncrushed loess, they broke significantly. But for the first-level pre-crushed loess, only a very small number of particles broke. Compared with the first-level pre-crushed loess, the particle breakage of the second-level pre-crushed sample can be negligible. It can be seen from the compression curves of the clayey loess, silty loess, and sandy loess, the compression curves of the second-level pre-crushed specimens are below the first-level pre-crushed specimens (Fig. 19). The input work is not higher than that in the early loading processes. Herein, no particle breakage occurred in the second-level pre-crushed specimen. The reason why there is little particle breakage in the first-level pre-crushed specimen may be that the reconstituting process changed the soil fabric and created new particle contacts. Clearly, little breakage happens in the second loading. There is no breakage in the third loading. Altuhafi and Coop (2011a) had shown that in one-dimensional compression, the breakage of sands would eventually cease as a fractal grading was approached. But in this study, the changes of grading required to stop breakage are much smaller.

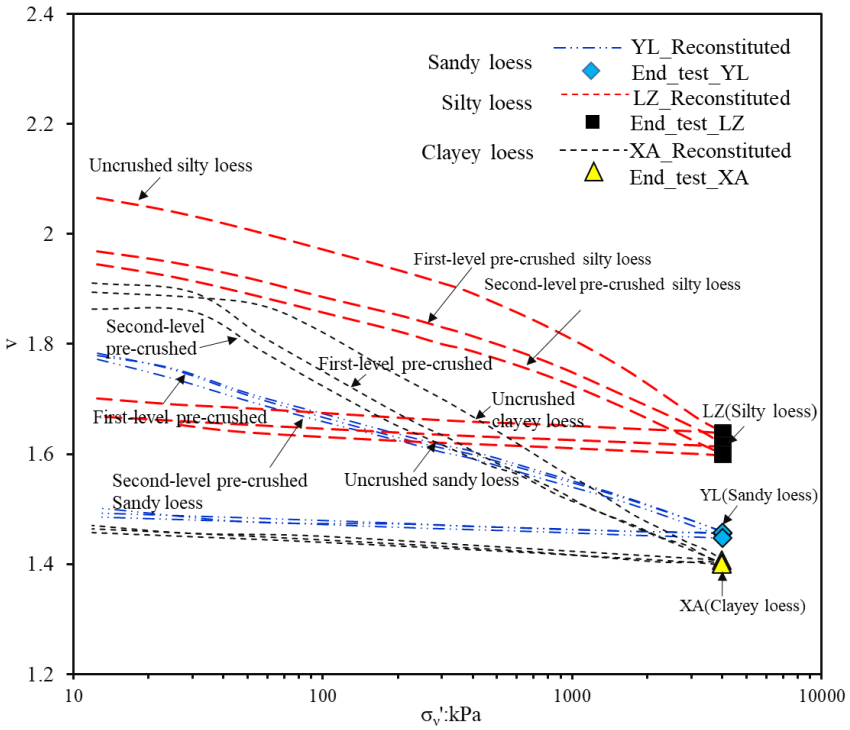

Fig. 19 Compression curves of the uncrushed and pre-crushed specimens after test

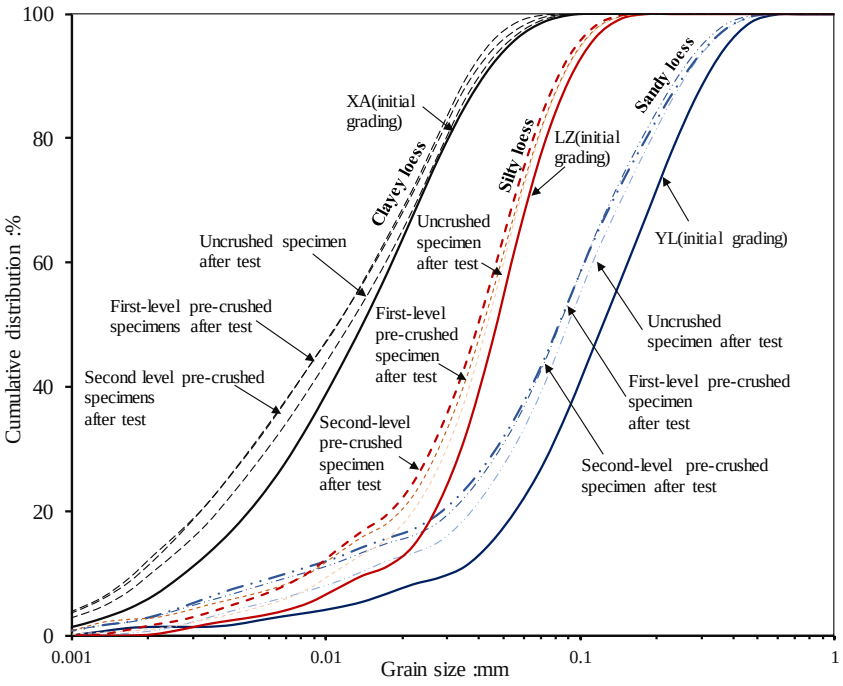

Fig. 20 PSD of uncrushed and pre-crushed specimens after test

4. Conclusions

An investigation of the one-dimensional compression behavior of sandy, silty, and clayey loess reveals that particle breakage does occur in all the samples, although the

particle breakage in sandy loess is much more than that in the silty and clayey loess. The initial stress for breakage is less than 0.5 MPa for the silty loess and clayey loess and around 2 MPa for the sandy loess. The breakage in the silty and clayey loess either ceases or reduces significantly with B_r reaching an approximately constant value when stress is larger than 2 MPa. The sandy loess did not reach a final degree of breakage even at the maximum vertical stress of 35 MPa. The particles in loose specimens were found to be subject to break easily than dense specimens. This mainly because that the loose specimens experienced a higher input work during one-dimensional loading. Pre-crushing dramatically reduced particle breakage. Only little particles broke in the first-level pre-crushed specimen but no particle breakage occurred in the second-level pre-crushed specimen.

Acknowledgements

The work was supported by the National Natural Science Foundation of China (Project No. 41772316), the Major Program of National Natural Science Foundation of China (Project No. 41790441), the National Key Research and Development Plan (Project No. 2018YFC1504701), the China Postdoctoral Science Foundation (Project No. 2019M663729) and the Youth Project of Natural Science Basic Research Plan in Shaanxi Province (Project No. 2020JQ-033).

Reference

1. Altuhafi, F.N., Coop, M.R., 2011a. Changes to particle characteristics associated with the compression of sands. Géotechnique, 61(6), 459-471.
2. Altuhafi, F.N., Coop, M.R., 2011b. The effect of mode of loading on the particle-

scale damage. Soils and Foundations, 51(5), 849-856.

3. Arasan, S., Akbulut, S., Hasiloglu, A.S., 2011. Effect of particle size and shape on the grain-size distribution using image analysis. International Journal of Structural Engneering, 1(4), 968-985.
4. Bandini, V., Coop, M.R., 2011. The influence of particle breakage on the location of the critical state line of sands. Soils and Foundations, 51, 591–600.
5. Bishop, A.W., 1966. The strength and soils as engineering materials. Géotechnique 16(2):91–130.
6. Coop, M.R., Sorensen, K.K., Freitas, T.B., et al. 2004. Particle breakage during shearing of a carbonate sand. Géotechnique, 54(3), 157-163.
7. Erzin, Y., Patel, A., Singh, D.N., et al. 2012. Factors influencing the crushing strength of some Aegean sands. Bulletin of Engineering Geology and the Environment,71(3), 529–536.
8. Erzin, Y., Yilmaz, I., 2008. Case study of crushing resistance of Anatolian sands at lower and higher density. Bulletin of Engineering Geology and the Environment, 67 (1), 71–77.
9. Feda, J., 2002. Notes on the effect of grain crushing on the granular soil behaviour. Engineering Geology, 63(1–2), 93–98.
10. Fu, Z., Chen, S., Peng, C., 2014. Modeling cyclic behavior of rockfill materials in a framework of generalized plasticity. International Journal of Geomechanics, 14, 191–204.
11. Ghafghazi, M., Shuttle, D.A., DeJong, J.T., 2014. Particle breakage and the critical state of sand. Soils and Foundations, 54, 451–461.
12. Hardin, B.O., 1985. Crushing of soil particles. Journal of Geotechnical Engineering, 111(10), 1177-1192.
13. Huang, J., Xu, S., Hu, S., 2014. Influence of particle breakage on the dynamic compression responses of brittle granular materials. Mechanics of Materials, 68:15–28.
14. Indraratna, B., Ionescu, D., Christie, H.D., 1998. Shear behavior of railway ballast based on large-scale triaxial tests. Journal of Geotechnical and Geoenvironmental Engineering, 124(5), 439-449.
15. Indraratna, B., Salim, W., 2002. Modelling of particle breakage of coarse aggregates incorporating strength and dilatancy. Proceedings of the Ice Geotechnical Engneering, 155(4), 243–252.

16. Lade, P.V., Yamamuro, J.A., Bopp, P.A., 1996. Significance of particle crushing in granular materials. Journal of Geotechnical and Geoenvironmental Engineering, 122(4):309–316.
17. Leung, C. F., Lee, F. H., Yet, N. S., 1996. The role of particle breakage in pile creep in sand. Canadian Geotechnical Journal, 33(6), 888-898.
18. Li, P.Y., Qian, H., Wu, J.H., 2014. Environment: Accelerate research on land creation. Nature, 510(7503), 29-31.
19. Liu M.C., Gao, Y.F., 2016. Constitutive modeling of coarse-grained materials incorporating the effect of particle breakage on critical state behavior in a framework of generalized plasticity. International Journal of Geomechanics, 17(5), 1-24.
20. Liu, T.S., 1985. Loess and the Environment. Science Press, Beijing (in Chinese).
21. McDowell, G.R., Bolton, M.D., 1998. On the micromechanics of crushable aggregates. Géotechnique, 48(5), 667-679.
22. McDowell, G.R., Bolton, M.D., Robertson, D., 1996. The fractal crushing of granular materials. Journal of the Mechanics and Physics of Solids, 44(12), 2079-2101.
23. Mehta, A. A., Patel, A., 2018. An investigation on the particle breakage of indian river sands. Engineering Geology, 233,23-37.
24. Nakata, Y., Hyde, A. F. L., Hyodo, M., et al. 1999. A probabilistic approach to sand particle crushing in the triaxial test. Géotechnique, 49(5), 567-583.
25. Peng, J.B., Wang, S., Wang, Q., et al. 2019. Distribution and genetic types of loess landslides in China, Journal of Asian Earth Sciences, 170, 329–350.
26. Shahnazari, H., Rezvani, R., 2013. Effective parameters for the particle breakage of calcareous sands: an experimental study. Engineering Geology, 159,98-105.
27. Sun, Y., Nimbalkar, S., Chen, C., 2019. Particle breakage of granular materials during sample preparation. Journal of rock mechanics and geotechnical engineering (in Chinese).
28. Takei, M., Kusakabe, O., Hayashi, T., 2001. Time-dependent behavior of crushed materials in one-dimensional compression tests. Soils and foundations, 41(1), 97-121.
29. Terzaghi K, Peck, R.B., 1948. Soil mechanics in engineering practice. Wiley, New York.
30. Valdes, J.R., Caban, B., 2006. Monitoring the hydraulic conductivity of crushing

sands. Geotechnical Testing Journal, 29 (4), 322–329.
31. Vilhar, G., Jovičić, V., Coop, M.R., 2013. The role of particle breakage in the mechanics of a non-plastic silty sand. Soils and Foundations, 53(1), 91-104.
32. Wang, X., Weng, Y., Wei, H., et al. 2019. Particle obstruction and crushing of dredged calcareous soil in the nansha islands, south china sea. Engineering Geology, 261, 105274.
33. Wood, D.M., Maeda, K., 2008. Changing grading of soil: effect on critical states. Acta Geotechnica, 3(1), 3-14.
34. Xiao, Y., Liu, H., Chen, Q., et al. 2017. Particle breakage and deformation of carbonate sands with wide range of densities during compression loading process[J]. Acta Geotechnica.
35. Xiao, Y., Yuan, Z., Chu, J., et al. 2019. Particle breakage and energy dissipation of carbonate sands under quasi-static and dynamic compression. Acta Geotechnica.
36. Yu, F., 2019. Particle breakage in granular soils: a review. Particulate Science and Technology,10.
37. Zhang, C., Chen, Q., Pan, Z., et al. 2019. Mechanical behavior and particle breakage of tailings under high confining pressure. Engineering Geology,265,105419.
38. Zhang, X., Baudet, B.A., Hu, W., et al. 2017. Characterisation of the ultimate particle size distribution of uniform and gap-graded soils. Soils and Foundations, 57(4), 603-618.

List of tables

List of figures